

Neutral Heteroleptic Lanthanide Complexes for Unravelling Host-Guest Assemblies in Organic Solvents: The Law of Mass Action Revisited.

Karine Baudet,[†] Vishal Kale,[†] Mohsen Mirzakhani,[†] Lucille Babel,[†] Soroush Naseri,[†] Céline Besnard,[§] Homayoun Nozary[†] and Claude Piguet^{†,*}

[§] *Laboratory of Crystallography, University of Geneva, 24 quai E. Ansermet, CH-1211 Geneva 4, Switzerland.*

[†] *Department of Inorganic and Analytical Chemistry, University of Geneva, 30 quai E. Ansermet, CH-1211 Geneva 4, Switzerland. Email: Claude.Piguet@unige.ch*

Supporting Information

(30 pages)

Experimental Section

All commercial chemicals were purchased from Sigma-Aldrich and Acros and used without further purification. The ligand **L1-L3**⁵ and lanthanide containers [La(hfa)₃dig], [La(tta)₃dig] and [La(pbta)₃dig]¹² were prepared following published procedures. Dichloromethane, diethyl ether and *N,N*-dimethylformamide were dried through alumina cartridges. Silica-gel plates (Merck, 60 F₂₅₄) were used for thin-layer chromatography, SiliaFlash[®] silica gel P60 (0.04-0.063 mm,) and Acros silica gel 60 (0.035-0.07 mm) was used for preparative column chromatography. Abbreviations: (dba)₂ = dibenzylideneacetone, P(Cy)₃ = tricyclohexylphosphine.

Analytic measurements. ¹H, ¹⁹F and ¹³C NMR spectra were recorded at different temperatures on Bruker Avance 400 MHz. Chemical shifts are given in ppm with respect to tetramethylsilane Si(CH₃)₄ (TMS). Pneumatically assisted electro-spray (ESI) mass spectra were recorded on an Applied Biosystems API 150EX (AB/MDS Sciex) equipped with a Turbo Ionspray source. Elemental Analyses were performed by K. L. Buchwalder from the Microchemical Laboratory of the University of Geneva.

X-Ray Crystallography. The selected crystal was mounted on a capton loop with protection oil. Cell dimensions and intensities were measured at 180 K on Supernova, Dual, Cu at zero Atlas diffractometer. Using Olex2,^{S1} the structure was solved with the ShelXT^{S2} structure position program using Intrinsic Phasing and refined with the ShelXL^{S3} refinement package using least squares minimization. Summary of crystal data, intensity measurement and structure refinements for [La(pbta)₃dig] were collected in Tables S3-S5.

- (S1) O. V. Dolomanov, O.V.; Bourhis, L. J.; Gildea, R.J.; Howard, J. A. K.; Puschmann H., OLEX2. A Complete Structure Solution, Refinement and Analysis Program. *J. Appl. Cryst.* **2009**, *42*, 339-341.
- (S2) Sheldrick, G. M., SHELXT–Integrated Space-Group and Crystal-Structure Determination *Acta. Cryst.* **2015**, *A71*, 3-8.
- (S3) Sheldrick, G. M., Crystal Structure Refinement with SHELXL. *Acta. Cryst.* **2015**, *C71*, 3-8.

Appendix 1. Derivation of equation (10).⁶

Following the classical procedure and regarding a simple association process:



In a solution i , the free energy change ΔG_i , can be expressed by chemical potentials

$$\Delta G_i = \mu_i^{\text{final}} - \mu_i^{\text{initial}} \quad (\text{A1-2})$$

With $\mu_i^{\text{initial}} = m\mu_i^{\text{L}} + n\mu_i^{\text{M}} + \mu_{\text{solv}}^{\text{initial}}$ and $\mu_i^{\text{final}} = \mu_i^{\text{L}_m\text{M}_n} + \mu_{\text{solv}}^{\text{final}}$.

Introduction of the usual expression of chemical potentials $\mu_X = \mu_X^0 + RT \ln(a_X)$, where μ_X^0 is the standard-state potential of the component X which takes into account its solvation state and a_X is the activity of component X, into equation (A1-2) gives (A1-3).

$$\Delta G_i = \left(\mu_{\text{L}_m\text{M}_n,i}^0 - m\mu_{\text{L},i}^0 + n\mu_{\text{M},i}^0 \right) + RT \ln \left[\frac{a_{\text{L}_m\text{M}_n,i}}{(a_{\text{L},i})^m (a_{\text{M},i})^n} \right] + \left(\mu_{\text{solv}}^{\text{final}} - \mu_{\text{solv}}^{\text{initial}} \right) \quad (\text{A1-3})$$

Combination of the three standard-state potentials delivers ΔG_i^0 :

$$\Delta G_i = \Delta G_i^0 + RT \ln \left[\frac{a_{\text{L}_m\text{M}_n,i}}{(a_{\text{L},i})^m (a_{\text{M},i})^n} \right] + \left(\mu_{\text{solv}}^{\text{final}} - \mu_{\text{solv}}^{\text{initial}} \right) \quad (\text{A1-4})$$

Setting the reference molar concentration at $c^0 = 1 \text{ M}$ and viewing activity coefficients of the solutes as unity: $a_{X,i} = \gamma_{X,i} (c_{X,i} / c^0) \rightarrow a_{X,i} \equiv c_{X,i}$

With these statements, rearrangement of (A1-4) gives:

$$\Delta G_i = \Delta G_i^0 + RT \ln(Q_{m,n,i}^{\text{L,M}}) + \left(\mu_{\text{solv}}^{\text{final}} - \mu_{\text{solv}}^{\text{initial}} \right) \quad (\text{A1-5})$$

Where $Q_{m,n,i}^{\text{L,M}} = \frac{c_{\text{L}_m\text{M}_n,i}}{(c_{\text{L},i})^m (c_{\text{M},i})^n}$ is the reaction quotient using molar concentration units.

At equilibrium $\Delta G_i = 0$ which transforms (A1-5) into (A1-6):

$$\Delta G_{m,n,\text{asso}}^{\text{L,M,0}} = -RT \ln(Q_{m,n,\text{asso},\text{eq}}^{\text{L,M}}) - \left(\mu_{\text{solv}}^{\text{final}} - \mu_{\text{solv}}^{\text{initial}} \right) \quad (\text{A1-6})$$

Under standard conditions, $\mu_{\text{solv}}^{\text{final}} = \mu_{\text{solv}}^{\text{initial}}$ and the classical van't Hoff equation is obeyed.

Whereas standard conditions imply the complete transformation of one mole of pure host and guest into one mole of pure complex, Castellano and Eggers considered that $\mu_{\text{solv}}^{\text{final}} \neq \mu_{\text{solv}}^{\text{initial}}$ when specific concentrations of host, guest and host-guest complexes coexist at equilibrium and assigned this deviation to a subpopulation of p solvent molecules in the reactants solvation shell (which are not taken into account in the chemical potential of the pure substances), which are released into the bulk

phase upon the formation of each molecule of complex $[\mathbf{L}_m\mathbf{M}_n]$, (i.e. the surface contact potential varies). Following this hypothesis, equilibrium (A1-1) becomes (A1-7).



The solvent potential is a complex function of hydrogen-bonding network and its own number density is relatively constant. Thus, the traditional expression of chemical potential for dissolved species is replaced⁶ with the notation $\mu_{\mathbf{S},i} = g_{\mathbf{S},i}^0 + \bar{g}_{\mathbf{S},i}$. The term $g_{\mathbf{S},i}^0$ is the solvent standard-state free energy per mole of solvent and $\bar{g}_{\mathbf{S},i}$ represents a specific P subset of solvent molecules released from the solvation shell $\bar{g}_{\mathbf{S}^{\text{contact},i}}$ to the bulk $\bar{g}_{\mathbf{S}^{\text{bulk},i}}$. Solvent is both a reactant and a product of the reaction, so

$g_{\mathbf{S},i}^0$ will remove from $\mu_{\text{solv}}^{\text{final}} - \mu_{\text{solv}}^{\text{initial}}$. Taking into account the stoichiometry of the association reaction, the total concentration per reference volume unit V^θ of the p subset solvent molecules is given by

$$P = p \cdot (c_{\mathbf{L}_m\mathbf{M}_n,i} / c^\theta) \quad (\text{A1-8})$$

Consequently, at equilibrium, equation (A1-6) transforms into (A1-9):

$$\Delta G_{m,n,\text{asso}}^{\mathbf{L},\mathbf{M}} = -RT \ln(Q_{m,n,\text{asso},\text{eq}}^{\mathbf{L},\mathbf{M}}) - p \cdot (c_{\mathbf{L}_m\mathbf{M}_n}^{\text{eq}} / c^\theta) (\bar{g}_{\mathbf{S}^{\text{bulk}}} - \bar{g}_{\mathbf{S}^{\text{contact}}}) \quad (\text{A1-9})$$

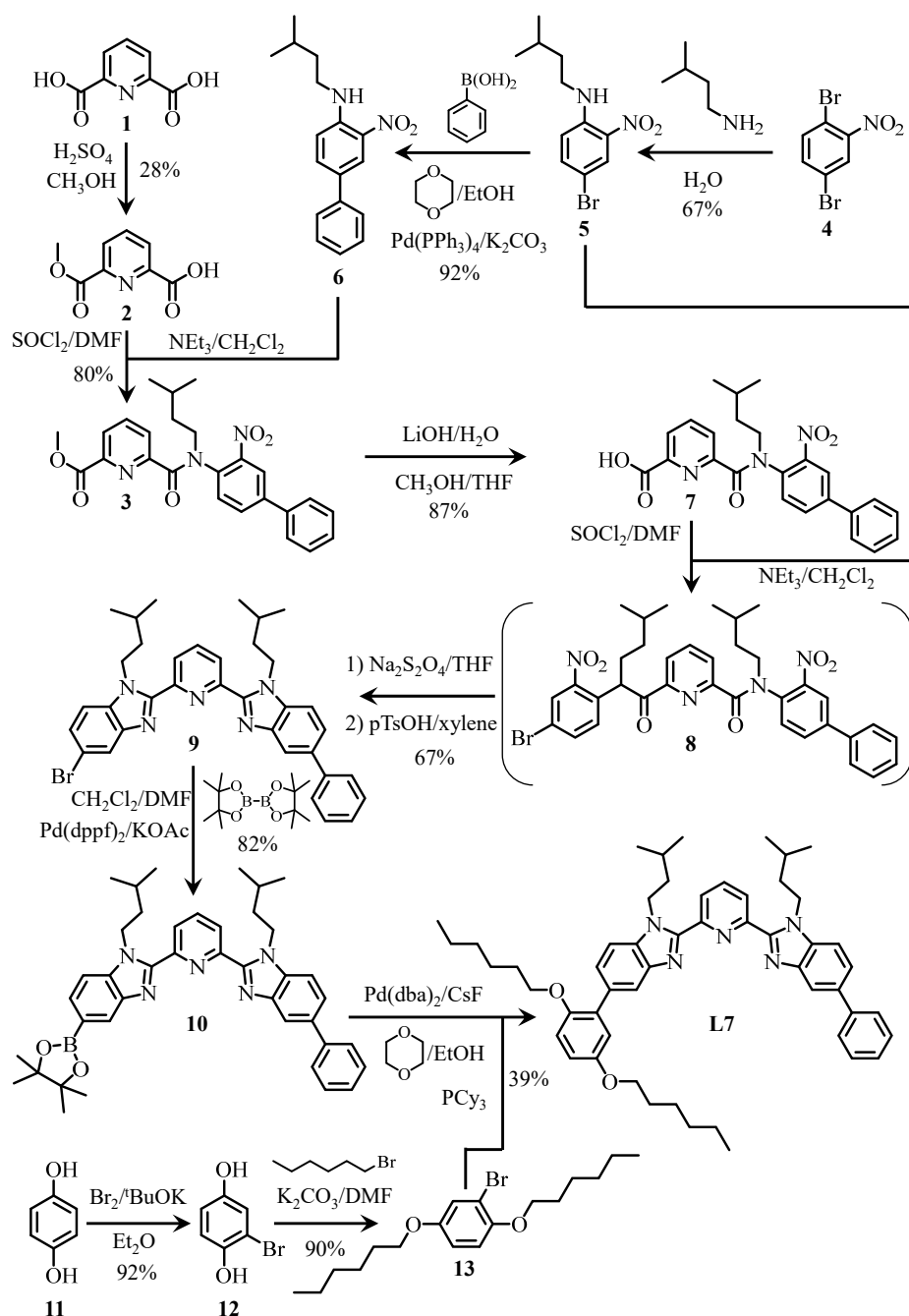
Introduction of the concept of desolvation free energy $\Delta G^{\mathbf{S}} = p(\bar{g}_{\mathbf{S}^{\text{bulk}}} - \bar{g}_{\mathbf{S}^{\text{contact}}})$ simplifies equation (A1-9)

$$\Delta G_{m,n,\text{asso}}^{\mathbf{L},\mathbf{M}} = -RT \ln(Q_{m,n,\text{asso},\text{eq}}^{\mathbf{L},\mathbf{M}}) - (c_{\mathbf{L}_m\mathbf{M}_n}^{\text{eq}} / c^\theta) \Delta G_{m,n,\text{asso}}^{\mathbf{L},\mathbf{M},\mathbf{S}} \quad (\text{A1-10})$$

Straightforward reorganization followed by a strict focus on a simple 1:1 complex $[\mathbf{LM}]$ yields the searched relationship:

$$-RT \ln(Q_{1,1,\text{asso},\text{eq}}^{\mathbf{L},\mathbf{M}}) = \Delta G_{1,1,\text{asso}}^{\mathbf{L},\mathbf{M}} + (c_{\mathbf{LM}}^{\text{eq}} / c^\theta) \Delta G_{1,1,\text{asso}}^{\mathbf{L},\mathbf{M},\mathbf{S}} \quad (10)$$

Appendix 2. Synthesis of ligand L7.



Scheme A2-1 Multistep synthesis of ligand **L7** with numbering scheme.

Preparation of 6-(methoxycarbonyl)picolinic acid (2).^{A2-1} 2,6-dipicolinic acid (**1**, 10.26 g, 60 mmol) and conc. sulfuric acid (1 mL) were refluxed in methanol/water (50 mL:50 mL) for 25 min. The resulting mixture was poured into sat. aq. NaHCO_3 (500 mL) and the aqueous phase was washed with dichloromethane (3x100 mL). The pH was then adjusted to pH 4 with aq. HCl and the aq. phase was extracted with dichloromethane (4x200 mL). The combined organic phases were dried over Na_2SO_4 , filtered and evaporated to dryness to give 6-(methoxycarbonyl)picolinic acid (**2**) as a white

powder. (3.1 g, yield 28%) $^1\text{H-NMR}$ (CDCl_3); 400 MHz), δ/ppm : 4.06 (s, 3H), 8.15 (t, 1H), 8.39 (d, 1H), 8.44 (s, 1H), 10.84 (br, 1H). ESI-MS (positive mode): m/z 181.82 $[\text{M}+\text{H}]^+$

Preparation of methyl 6-(isopentyl(3-nitro-[1,1'-biphenyl]-4 yl) carbamoyl)picolinate (3). Thionyl chloride (16.3 mL, 57 g, 22.4 mmol), 6-(methoxycarbonyl)picolinic acid (**2**, 2.0 g, 11.2 mmol) and *N,N*-dimethylformamide (2 drops) were refluxed (80 °C) under an inert atmosphere for 1h. Evaporation to dryness followed by drying under vacuum provided a white solid, which was dissolved in dry dichloromethane (30 mL). Dichloromethane (25 mL) containing *N*-isopentyl-3-nitro-[1,1'-biphenyl]-4-amine (**6**, 3.5 g, 12.3 mmol) and triethyl amine (4 mL) was slowly added and the mixture refluxed overnight. After evaporation to dryness, the residue was partitioned between dichloromethane (200 mL) and half-sat. aq. NH_4Cl (200 mL). The aq. phase was separated, extracted with dichloromethane (2x100 mL) and the combined organic phases were dried (Na_2SO_4), filtered and evaporated to dryness. The residual oil was purified by column chromatography (Silicagel, $\text{CH}_2\text{Cl}_2/\text{MeOH}$ 100:0 \rightarrow 99:1) to yield methyl 6-(isopentyl(3-nitro-[1,1'-biphenyl]-4 yl) carbamoyl)picolinate (**3**, 4.03 g, 9.0 mmol, 80%) as a yellow oil. $^1\text{H-NMR}$ (400 MHz, CDCl_3 , major rotamer within a 7:1 mixture of two rotamers) δ 8.23 (s, 1H), 8.13 (d, $J = 7.8$ Hz, 1H), 7.97 (d, $J = 7.8$ Hz, 1H), 7.87 (t, $J = 7.8$ Hz, 1H), 7.82 (d, $J = 8.2$ Hz, 1H), 7.61 (d, $J = 7.4$ Hz, 2H), 7.56-7.43 (m, 4H), 4.31-4.17 (m, 1H), 3.77-3.67 (m, 1H), 3.73 (s, 3H), 1.76-1.52 (m, 3H), 0.97 (t, $J = 7.2$ Hz, 6H). ESI-MS (positive mode): m/z 448.3 $[\text{M}+\text{H}]^+$.

Preparation of 4-bromo-*N*-isopentyl-2-nitroaniline (5).^{A2-2} 1,4-dibromo-2-nitrobenzene (**4**, 5.0 g, 17.8 mmol) and isopentylamine were heated at 110 °C for 24h in a sealed vessel. The resulting red solution was concentrated by evaporation and partitioned between dichloromethane (250 mL) and half sat. aq. NH_4Cl (250 mL). The aqueous phase was extracted with dichloromethane (3x100 mL). The combined organic phases were dried (Na_2SO_4), filtered and evaporated to dryness to give 4-bromo-*N*-isopentyl-2-nitroaniline as red crystals (**5**, 3.5 g, 67%). $^1\text{H-NMR}$ (400 MHz, CDCl_3), δ/ppm : 1.00 (d, 6H), 1.65 (q, 2H), 1.78 (m, 1H), 3.31 (q, 2H), 6.78 (d, 1H), 7.50 (dd, 1H), 8.01 (s, 1H), 8.34 (d, 1H). ESI-MS (positive mode): m/z 288.9 $(\text{M}+\text{H})^+$.

Preparation of *N*-isopentyl-3-nitro-[1,1'-biphenyl]-4-amine (6). 4-bromo-*N*-isopentyl-2-nitroaniline (**5**, 6.32 g, 22.0 mmol), phenylboronic acid (3.22 g, 26.4 mmol, 1.2 eq.), K_2CO_3 (15.20 g, 110.0 mmol, 5.0 eq.), and tetrakis(triphenylphosphine) palladium(0) (508 mg, 0.44 mmol, 0.02 eq.) were introduced into a Schlenk tube, which was flushed with argon. A degassed mixture of dioxane (36 mL) and ethanol (24 mL) was added, and the Schlenk was heated at 100 °C for 24h. After evaporation to dryness, the solid was partitioned between Na_2CO_3 half sat. (150 mL) and dichloromethane (200 mL). The aq. phase was extracted with dichloromethane (2x 200 mL). The combined organic phases were dried over Na_2SO_4 , filtered and evaporated to dryness. The dark red

solid was filtered through a pad of silica using hexane/CH₂Cl₂ 60:40 as the eluent. The resulting red solid was finally crystallized from a mixture of CH₂Cl₂ and hexane to get *N*-isopentyl-3-nitro-[1,1'-biphenyl]-4-amine as orange-red crystals (**6**, 5.80 g, 92%). ¹H-NMR (400 MHz, CDCl₃): δ 8.47 (d, *J* = 2.2 Hz, 1H), 8.09 (br s, 1H), 7.75 (dd, *J* = 8.9, 2.2 Hz, 1H), 7.59 (d, *J* = 7.5 Hz, 2H), 7.46 (t, *J* = 7.4 Hz, 2H), 7.35 (t, *J* = 7.4 Hz, 1H), 6.97 (d, *J* = 8.9 Hz, 1H), 3.39 (td, *J* = 7.1, 5.4 Hz, 3H), 1.82 (non, *J* = 6.7 Hz, 1H), 1.69 (q, *J* = 7.1 Hz, 2H), 1.03 (d, *J* = 6.6 Hz, 5H). ESI-MS (positive mode, CH₂Cl₂): *m/z* 284.9 (M+H)⁺, 569.3 (2M+H)⁺.

Preparation of 6-(isopentyl(3-nitro-[1,1'-biphenyl]-4-yl)carbamoyl)picolinic acid (7). A solution of LiOH·H₂O (1.99 g, 47.5 mmol) in methanol/water (80 mL: 20 mL) was added dropwise to a cooled (0 °C) solution of the ester methyl 6-(isopentyl(3-nitro-[1,1'-biphenyl]-4-yl)carbamoyl)picolinate (**3**, 4.26 g, 9.5 mmol) in THF (30 mL). The mixture was stirred for 3h at 0 °C, neutralized with 1M aq. hydrochloric acid and evaporated to remove THF and methanol. The resulting mixture is extracted with dichloromethane (3x 100 mL). The combined organic phases were dried over Na₂SO₄, filtered and evaporated to dryness to obtain 6-(isopentyl(3-nitro-[1,1'-biphenyl]-4-yl)carbamoyl)picolinic acid as an orange powder (**7**, 3.60 g, 8.31 mmol, 87%). ¹H-NMR (400 MHz, CDCl₃, major rotamer within a 14:1 mixture of two rotamers): δ/ppm: 8.23 (d, *J* = 7.8 Hz, 1H), 8.13 (d, *J* = 7.7 Hz, 1H), 8.08 (s, 1H), 8.01 (t, *J* = 7.8 Hz, 1H), 7.84 (d, *J* = 8.2 Hz, 1H), 7.58 (d, *J* = 7.6 Hz, 2H), 7.55 – 7.41 (m, 4H), 4.27-4.14 (m, 1H), 3.84-3.71 (m, 1H), 1.77-1.57 (m, 4H), 0.98 (t, *J* = 6.1 Hz, 6H). ESI-MS (positive mode, CH₂Cl₂): *m/z* 433.8 [M+H]⁺.

Preparation of 5-bromo-1-isopentyl-2-(6-(1-isopentyl-5-phenyl-1H-benzo(d)imidazo-2-yl)pyridine-2-yl)-1H-benzo(d)imidazole (9).^{A2-3} Thionyl chloride (4.5 mL, 61.3 mmol), 6-(isopentyl(3-nitro-[1,1'-biphenyl]-4-yl)carbamoyl)picolinic acid (**7**, 1.329 g, 3.1 mmol) and THF (4 drops) were refluxed (80 °C) under an inert atmosphere for 1h. Evaporation to dryness followed by drying under vacuum provided a pale yellow solid, which was dissolved in dry THF (1.5 mL). 4-bromo-*N*-isopentyl-2-nitroaniline (**5**, 0.964 g, 3.4 mmol) in THF (2.5 mL) was slowly added and the mixture heated at 80 °C overnight. The formation of the intermediate product **8** was checked with TLC and mass spectroscopy (ESI-MS positive mode: *m/z* 703.8 [M+H]⁺) and the solution evaporated to dryness under vacuum. Sodium dithionite (2.0 g, 11.5 mmol) in deionized water/methanol (10 mL :2 mL) was slowly added under N₂ at room temperature upon magnetic stirring to a solution of intermediate **8** in THF (10 mL). The resulting mixture was stirred for 18h at RT. Dichloromethane (10 mL) and 10% aq. NaHCO₃ (5 mL) were added, stirred at RT for 1h (pH adjusted to 6.5-7). The organic layer was separated, washed with saturated brine (10 mL), dried over anhydrous Na₂SO₄ and the solvent was distilled off under reduced pressure. Xylene (10 mL) and para-toluene sulfonic acid (0.5 g, 2.9 mmol) were added and the resulting mixture was refluxed at 140 °C for 24 h. After cooling,

the final was pH adjusted to 7-8 with aq. 10% K₂CO₃ solution and the aq. phase extracted with dichloromethane (100 mL and 3x150 mL). The combined organic layers were dried over sodium sulfate, filtered and evaporated to dryness to give a yellowish oil. The residual oil was purified by column chromatography (Silicagel, CH₂Cl₂:MeOH, 99.5:0.5) yielded 5-bromo-1-isopentyl-2-(6-(1-isopentyl-5-phenyl-1H-benzo(d)imidazo-2-yl)pyridine-2-yl)-1H-benzo(d)imidazole as a white solid (**9**, 1.26 g, 67%). ¹H-NMR (400 MHz, CDCl₃), δ/ppm: 8.37 (dd, *J* = 7.9, 1.0 Hz, 1H), 8.30 (dd, *J* = 7.9, 1.0 Hz, 1H), 8.11 (t, *J* = 7.9 Hz, 2H), 8.10 (d, *J* = 1.2 Hz, 1H), 8.03 (d, *J* = 1.6 Hz, 1H), 7.71 (d, *J* = 7.5 Hz, 2H), 7.65 (dd, *J* = 8.5, 1.6 Hz, 1H), 7.54 (d, *J* = 8.8 Hz, 1H), 7.51 (t, *J* = 7.8 Hz, 2H), 7.49 (dd, *J* = 8.6, 1.9 Hz, 1H), 7.39 (t, *J* = 7.4 Hz, 1H), 7.36 (d, *J* = 8.6 Hz, 1H), 4.79-4.67 (m, 4H), 1.73-1.57 (m, 4H), 1.50-1.33 (m, 2H), 0.74 (d, *J* = 6.8 Hz, 6H), 0.72 (d, *J* = 6.8 Hz, 6H). ESI-MS (positive mode): *m/z* 607.8 [M+H]⁺.

Preparation of 5-(2,5-bis(hexyloxy)phenyl)-1-isopentyl-2-(6-(1-isopentyl-5-phenyl-1H-benzo[d]imidazol-2-yl)pyridin-2-yl)-1H-benzo[d]imidazole (L7). 5-bromo-1-isopentyl-2-(6-(1-isopentyl-5-phenyl-1H-benzo(d)imidazo-2-yl)pyridine-2-yl)-1H-benzo(d)imidazole (**9**, 651 mg, 1.07 mmol, 1.0 eq.), pinacoldiborane (328 mg, 1.29 mmol, 1.2 eq.), KOAc (216 mg, 3.22 mmol, 3.0 eq.), and [1,1'-bis(diphenylphosphino)ferrocene]dichloropalladium(II) with dry dichloromethane (26 mg, 0.03 mmol, 0.03 eq.) were introduced into a Schlenk tube, which was flushed with argon. Degassed DMF (7 mL) was added to the Schlenk, which was then heated at 80 °C for 72h. Half. sat. NaCl (150 mL) was added and this aq. phase was extracted with diethyl ether (4x100 mL). The combined organic phases were dried over Na₂SO₄, filtered and evaporated to dryness. The brown oil was purified by column chromatography (Silicagel, CH₂Cl₂/MeOH 100:0→98:2) to yield 89% of the reactive intermediate **10** as a yellow oil (625 mg, 0.96 mmol). ESI-MS (positive mode): *m/z* 654.5 [M+H]⁺. A mixture of 2-bromo-1,4-dihexyloxybenzene (**13**, 500 mg, 1.24 mmol), intermediate **10** (296 mg, 0.45 mmol), cesium fluoride (78 mg, 5.15 mmol), Pd(dba)₂ (30 mg, 0.05 mmol) and P(Cy)₃ (15 mg, 0.05 mmol) were introduced into a Schlenk tube previously flushed with nitrogen. A solution of degassed dioxane (40 mL) and ethanol (25 mL) was added and the reaction mixture was stirred for 24h under reflux. After extraction with CH₂Cl₂ (50 mL), the product was purified by column chromatography (Silicagel, CH₂Cl₂/MeOH 100:0→100:0.5) to give 39% of pure 5-(2,5-bis(hexyloxy)phenyl)-1-isopentyl-2-(6-(1-isopentyl-5-phenyl-1H-benzo[d]imidazol-2-yl)pyridin-2-yl)-1H-benzo[d]imidazole as a white powder (**L7**, 141 mg, 0.18 mmol). ¹H-NMR (400 MHz, CDCl₃), δ/ppm: 8.36 (dd, *J* = 7.9, 1.0 Hz, 2H), 8.11 (t, *J* = 7.9 Hz, 1H), 8.08 (s, 1H), 7.72 (d, *J* = 7.9 Hz, 2H), 7.66 (d, *J* = 7.9 Hz, 1H), 7.63 (d, *J* = 7.9 Hz, 1H), 7.53 (s, 1H), 7.51 (d, *J* = 7.9 Hz, 2H), 7.49 (t, *J* = 7.9 Hz, 2H), 7.39 (t, *J* = 7.9 Hz, 1H), 7.04 (d, *J* = 1.4 Hz, 1H), 6.97 (s, 1H), 6.88 (d, *J* = 7.9 Hz, 1H), 4.77 (m, 4H), 4.00 (t, *J* = 6.9 Hz, 2H), 3.93 (t, *J* = 6.9 Hz, 2H), 1.81 (m, 2H), 1.68 (m, 4H), 1.70 (m,

2H), 1.48 (m, 4H), 1.37 (m, 8H), 1.27 (m, 2H), 0.94 (t, $J = 6.8$ Hz, 3H), 0.86 (t, $J = 6.8$ Hz, 3H), 0.75 (dd, $J = 6.8$ Hz, 12H). ESI-MS (positive mode) : m/z 805.8 $[M+H]^+$, 1610.2 $[2M+H]^+$

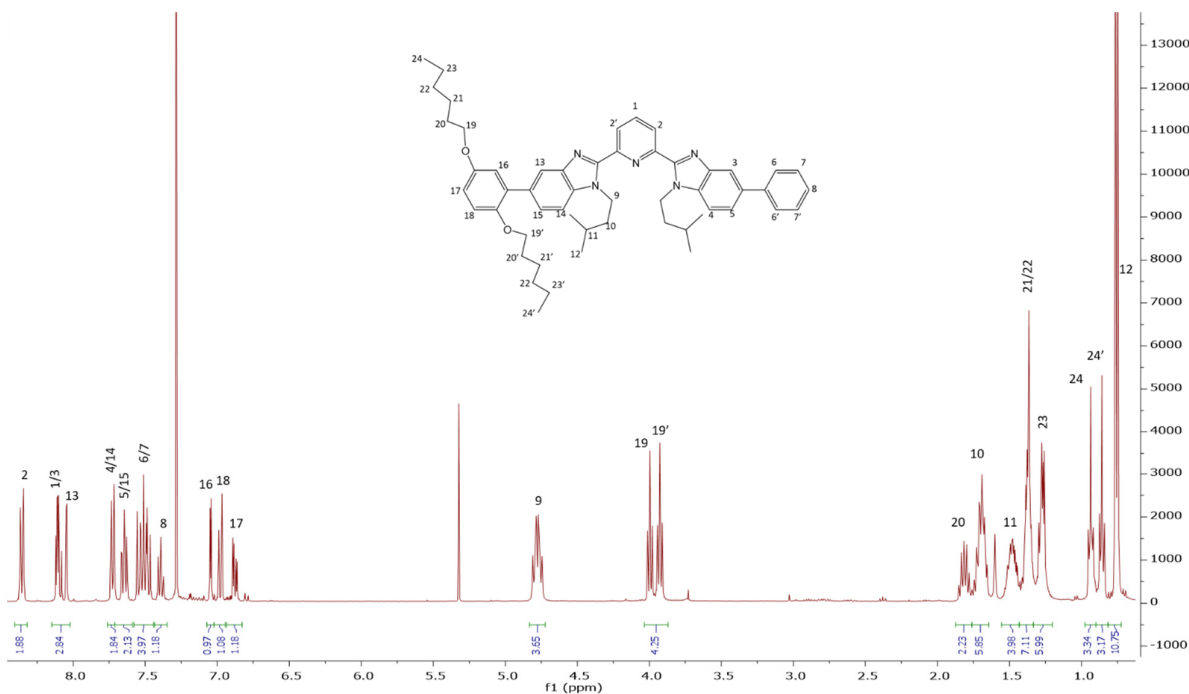


Figure A2-1 $^1\text{H-NMR}$ spectrum of pure ligand L7 with numbering scheme.

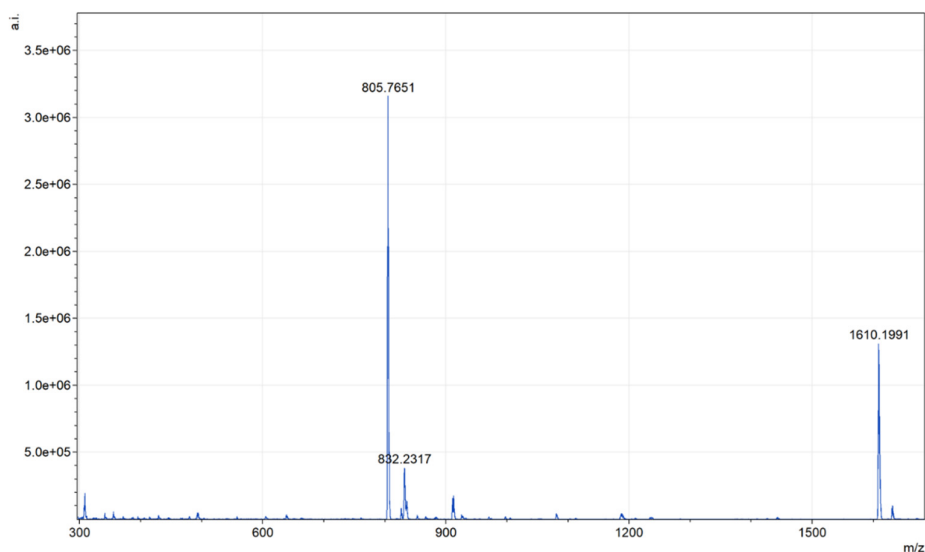


Figure A2-2 ESI-MS (positive mode) of ligand L7.

Preparation of bromohydroquinone (12). A solution of bromine (2.30 mL, 45.4 mmol) was added dropwise to a mixture of hydroquinone (**11**, 5.00 g, 45.4 mmol) and potassium tert-butoxide (5.10 g, 45.4 mmol) in diethyl ether (30 mL) at 0 °C. The reaction mixture was stirred two hours at room temperature. The solution was then quenched by using aqueous sodium solution (10%) and extracted with Et₂O. The organic layers were collected, washed with water and brine, dried over anhydrous Na₂SO₄ and concentrated under vacuum. The crude compound was purified by flash column

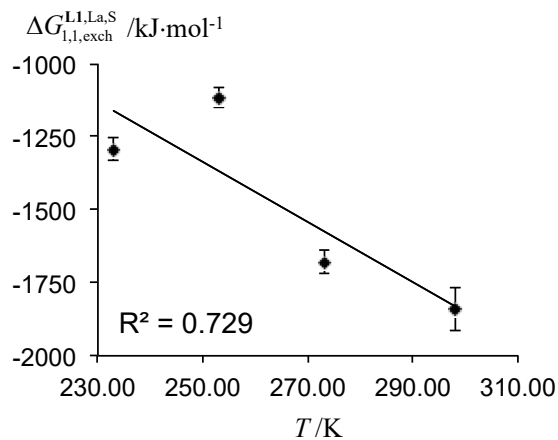
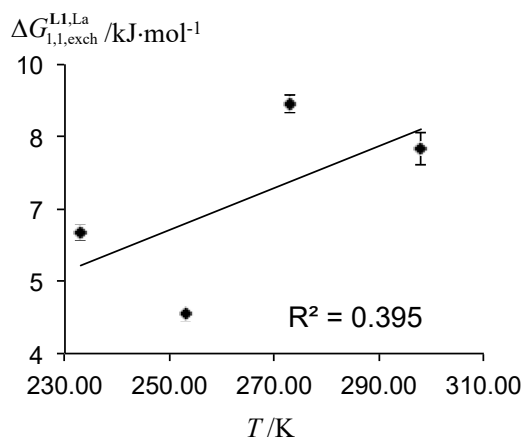
chromatography (SiO₂, Hexane/EtOAc 9:1) to give the bromohydroquinone (**12**, 7.90 g, 92%) as a white powder. ¹H-NMR (CDCl₃; 400 MHz), δ/ppm: 6.99 (d; ⁴J = 2.9 Hz, 1H), 6.90 (d; ³J = 8.8 Hz, 1H), 6.73 (dd; ³J = 8.8 Hz, ⁴J = 2.9 Hz, 1H).

Preparation of 2-bromo-1,4-dihexyloxybenzene (13). To a mixture of 1-bromohexane (7.50 mL, 52.91 mmol), K₂CO₃ (7.31 g, 52.91 mmol) and 18-Crown-6 (10 mg, 0.04 mmol) previously flushed into inert atmosphere, a solution of bromohydroquinone (**12**, 1.00 g, 5.29 mmol) in DMF (20 mL) was added. The reaction mixture was stirred for 24 h. under reflux (110 °C). Solvents were removed and the crude product was extracted with ethyl acetate (3x30 mL), washed with water, dried over anhydrous Na₂SO₄, filtered and concentrated under reduce pressure. Purification by flash column chromatography (SiO₂, Hexane/CH₂Cl₂ = 100:1 → 10:1) gave pure 2-bromo-1,4-dihexyloxybenzene (**13**, 1.70 g, 90%) as a yellow oil. ¹H-NMR (CDCl₃; 400 MHz), δ/ppm: 7.11 (d; 1H), 6.82 (d; 1H), 6.78 (dd; ³J = 8.8 Hz, 1H), 3.95 (t; ³J = 6.5 Hz, 2H), 3.88 (t; ³J = 6.5 Hz, 2H), 1.77 (sext; ³J = 7.2 Hz, 4H), 1.47 (m; ³J = 7.2 Hz, 4H), 1.34 (m; 8H), 0.91 (t; ³J = 6.2 Hz, 6H).

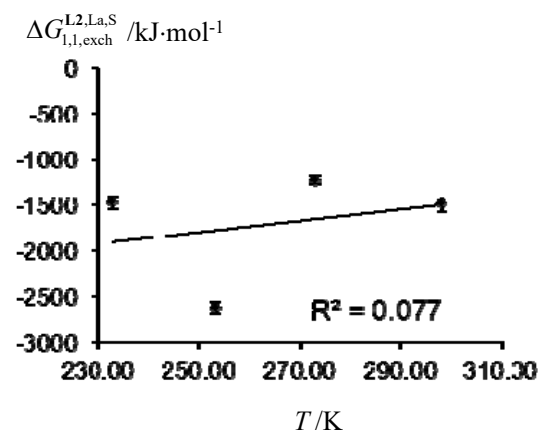
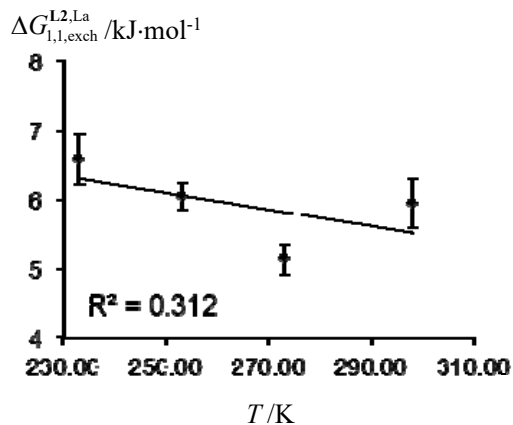
References

- A2-1 Lemonnier, J.-F.; Guénée, L.; Beuchat, C.; Wesolowski, T. A.; Mukherjee, P.; Waldeck, D. H.; Gogik, K. A.; Petoud, S.; Piguet, C., Optimizing Sensitization Processes in Dinuclear Luminescent Lanthanide Oligomers: Selection of Rigid Aromatic Spacers. *J. Am. Chem. Soc.* **2011**, *133*, 16219-16234.
- A2-2 Zaïm, A.; Nozary, H.; Guénée, L.; Besnard, C.; Lemonnier, J.-F.; Petoud, S.; Piguet, C., N-heterocyclic Tridentate Aromatic Ligands Bound to [Ln(hfac)₃] Units: Thermodynamic, Structural and Luminescent Properties. *Chem. Eur. J.* **2012**, *18*, 7155-7168.
- A2-3 <https://www.google.com/patents/CN105399683A?cl=en>

a) L1, 0 M added diglyme



b) L2, 0 M added diglyme



c) L3, 0 M added diglyme

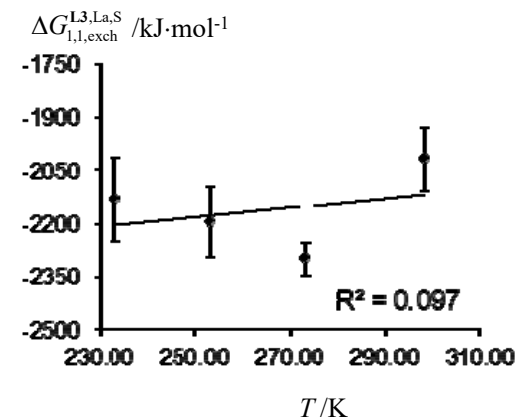
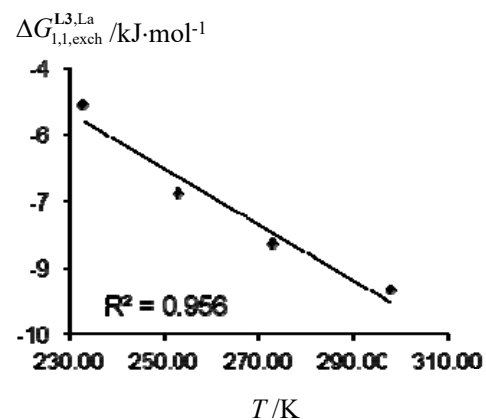


Figure S1 Van't Hoff plots for $\Delta G_{1,1,exch}^{Lk,La}$ (left part) and $\Delta G_{1,1,exch}^{Lk,La,S}$ (right part) measured for the titrations of L1-L3 with $[\text{La}(\text{hfac})_3(\text{dig})]$ (Equilibrium 6) in CD_2Cl_2 at variable temperatures.

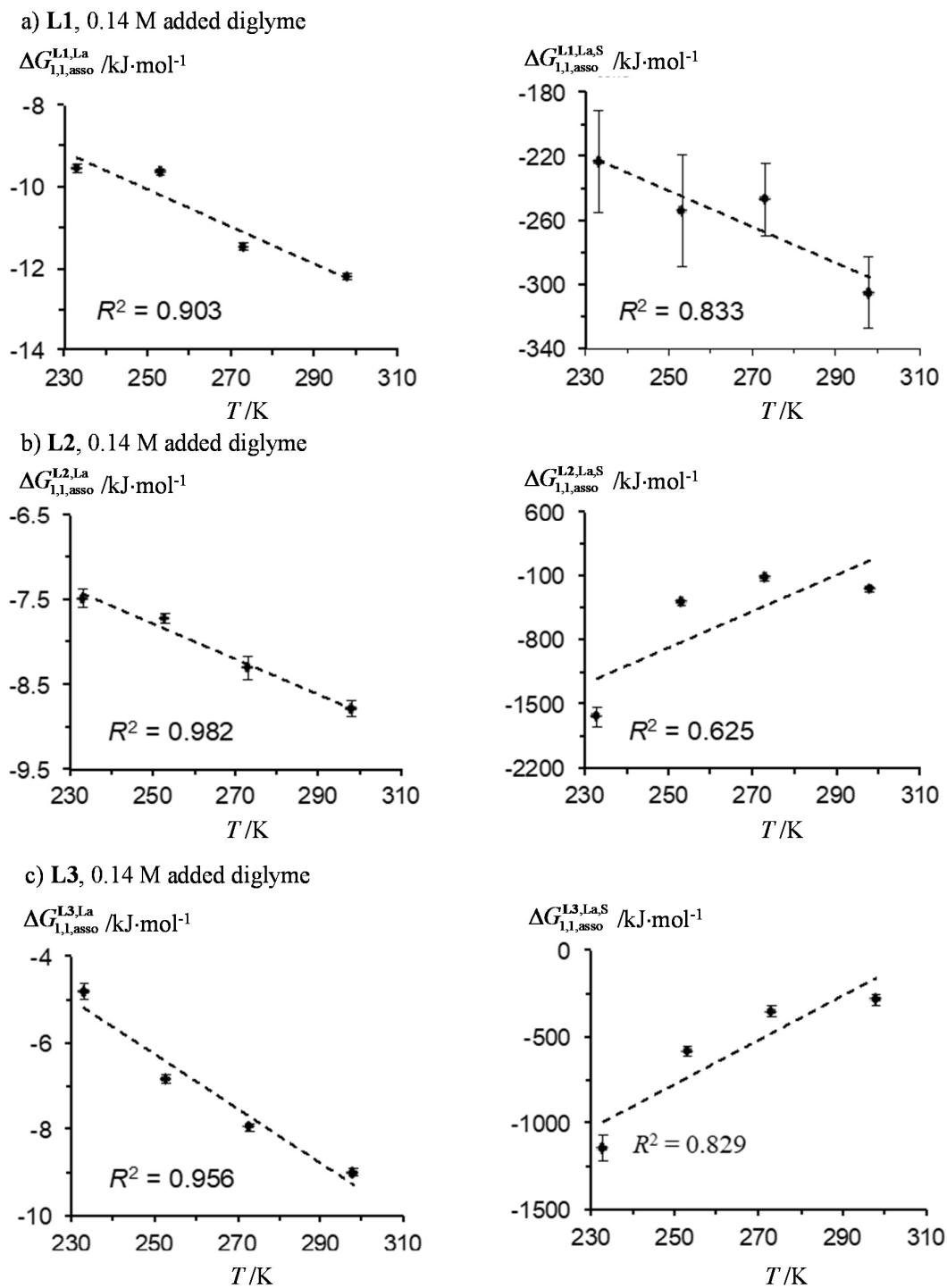


Figure S2 Van't Hoff plots for $\Delta G_{1,1,asso}^{Lk,La}$ (left part) and $\Delta G_{1,1,asso}^{Lk,La,S}$ (right part) measured for the titrations of L1-L3 with $[\text{La}(\text{hfac})_3(\text{dig})]$ (Equilibrium 7) in $\text{CD}_2\text{Cl}_2 + 0.14 \text{ M diglyme}$ at variable temperatures.

Table S1 Thermodynamic Parameters $\Delta H_{1,1,\text{exch}}^{\text{Lk,L a}}$, $\Delta H_{1,1,\text{exch}}^{\text{Lk,L a,S}}$, $\Delta S_{1,1,\text{exch}}^{\text{Lk,L a}}$, $\Delta S_{1,1,\text{exch}}^{\text{Lk,L a,S}}$ Determined for the Titrations of **L1-L3** with [La(hfac)₃(dig)] (Equilibrium 6) in CD₂Cl₂.^a

Ligands	$\Delta H_{1,1,\text{exch}}^{\text{Lk,L a}}$	$\Delta S_{1,1,\text{exch}}^{\text{Lk,L a,S}}$	$\Delta H_{1,1,\text{exch}}^{\text{Lk,L a,S}}$	$\Delta S_{1,1,\text{exch}}^{\text{Lk,L a,S}}$
	/kJ·mol ⁻¹	/J·mol ⁻¹ ·K ⁻¹	/kJ·mol ⁻¹	/J·mol ⁻¹ ·K ⁻¹
L1	2.3 (11.9)	-15 (45)	419 (1230)	6984 (4633)
L2	8.8 (3.3)	12 (13)	-3393 (4032)	-6354 (15195)
L3	17.2 (6.9)	42 (26)	-2514 (758)	-1327 (2858)

^a The reported uncertainties are those calculated using linear least-square techniques.

Table S2 Thermodynamic Parameters $\Delta H_{1,1,\text{asso}}^{\text{Lk,L a}}$, $\Delta H_{1,1,\text{asso}}^{\text{Lk,L a,S}}$, $\Delta S_{1,1,\text{asso}}^{\text{Lk,L a}}$, $\Delta S_{1,1,\text{asso}}^{\text{Lk,L a,S}}$ Determined for the Titrations of **L1-L3** with [La(hfac)₃(dig)] (Equilibrium 7) in CD₂Cl₂ + 0.14 M diglyme.^a

Ligands	$\Delta H_{1,1,\text{asso}}^{\text{Lk,L a}}$	$\Delta S_{1,1,\text{asso}}^{\text{Lk,L a}}$	$\Delta H_{1,1,\text{asso}}^{\text{Lk,L a,S}}$	$\Delta S_{1,1,\text{asso}}^{\text{Lk,L a,S}}$
	/kJ·mol ⁻¹	/J·mol ⁻¹ ·K ⁻¹	/kJ·mol ⁻¹	/J·mol ⁻¹ ·K ⁻¹
L1	1.4 (2.8)	46 (10)	40 (94)	1128 (357)
L2	-2.6 (5)	21 (2)	-5826 (2875)	19761 (10834)
L3	9.5 (2.5)	63 (10)	-3979 (1093)	-12813 (4119)

^a The reported uncertainties are those calculated using linear least-square techniques.

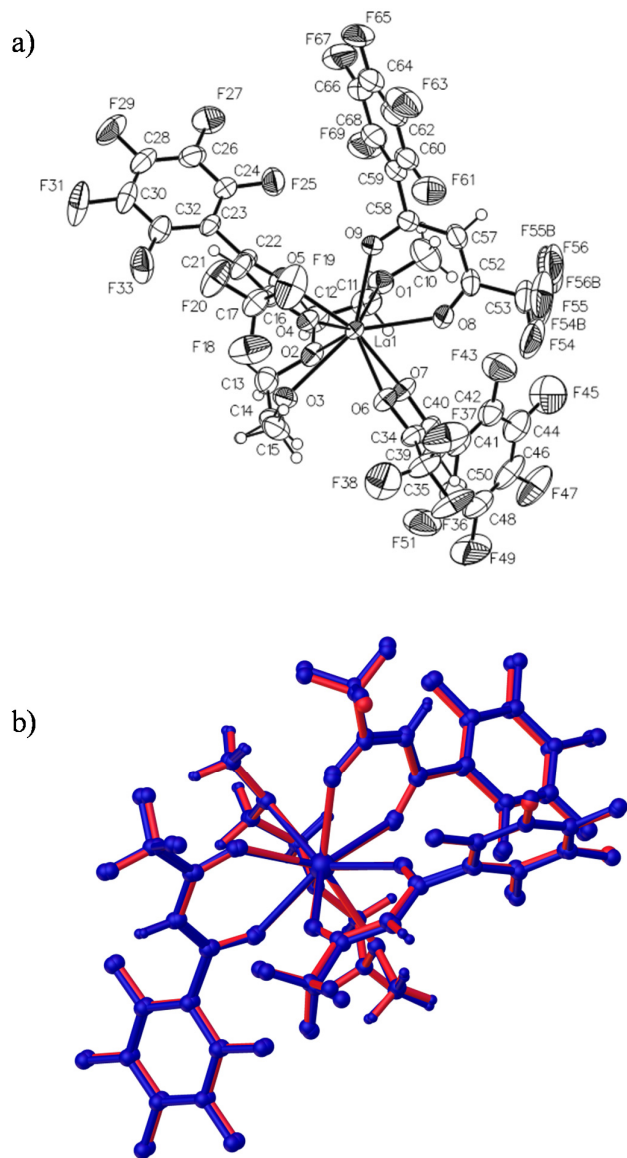


Figure S3 a) ORTEP molecular view of [La(pbta)₃(dig)] in the crystal structure with numbering scheme (thermal ellipsoids are drawn at 50% probability level and hydrogen atoms are omitted for clarity). b) Superimposition of the molecular structures of [La(pbta)₃(dig)] (blue) and [Eu(pbta)₃(dig)]¹² (red) in their X-ray crystal structures.

Table S3 Summary of Crystal Data, Intensity Measurements and Structure Refinements for [La(pbta)₃(dig)].

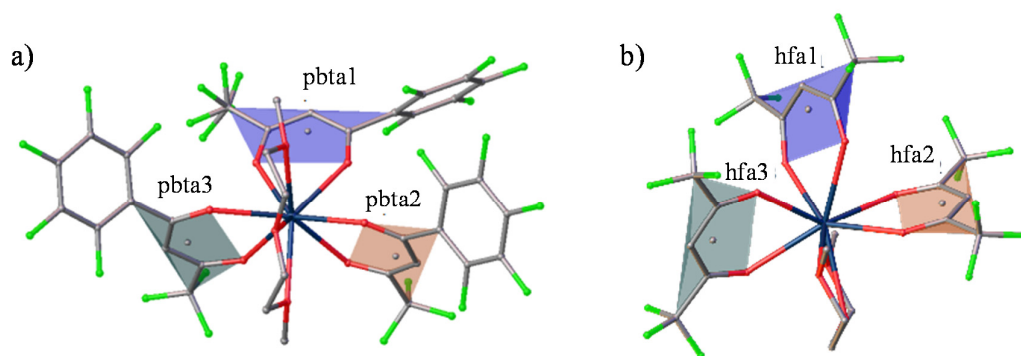
Empirical formula	C ₃₆ H ₁₇ F ₂₄ LaO ₉	
Formula weight	1188.41	
Temperature	180(10) K	
Wavelength	1.54184	
Crystal system	monoclinic	
Space group	<i>P2₁/c</i>	
Unit cell dimensions	<i>a</i> = 8.2940(3) Å	<i>α</i> = 90°
	<i>b</i> = 27.8547(9) Å	<i>β</i> = 101.943(4) °
	<i>c</i> = 19.0060(8) Å	<i>γ</i> = 90°
Volume	4295.9(3) Å ³	
<i>Z</i>	4	
Density (calculated)	1.837 g/cm ³	
Absorption coefficient	9.147 mm ⁻¹	
<i>F</i> (000)	2312.0	
Crystal size	0.685 × 0.096 × 0.028 mm ³	
Radiation	CuKα (<i>λ</i> = 1.54184 Å)	
Theta range for data collection	6.346 to 148.076°	
Index ranges	-10 ≤ <i>h</i> ≤ 10, -33 ≤ <i>k</i> ≤ 22, -21 ≤ <i>l</i> ≤ 23	
Reflections collected	19789	
Independent reflections	8469 [<i>R</i> _{int} = 0.0414, <i>R</i> _{sigma} = 0.0422]	
Completeness to theta = 74.038°	97.0%	
Absorption correction	Gaussian	
Max. and min. transmission	1.000 and 0.660	
Refinement method	Least Squares minimisation	
Data/restraints/parameters	8469/18/661	
Goodness-of-fit on <i>F</i> ²	1.025	
Final <i>R</i> indices [<i>I</i> ≥ 2σ(<i>I</i>)]	<i>R</i> ₁ = 0.0442, w <i>R</i> ₂ = 0.1238	
<i>R</i> indices (all data)	<i>R</i> ₁ = 0.0516, w <i>R</i> ₂ = 0.1293	
Largest diff. Peak and hole	1.10 and -0.70 e·Å ⁻³	

Table S4 Selected Bond Distances (Å), Bond Angles (°) in [La(pbta)₃(dig)].

Bond Distances / Å					
Atoms 1-2	Distance	Atoms 1-2	Distance	Atoms 1-2	Distance
La-O1	2.618(3)	La-O4	2.472(3)	La-O7	2.495(3)
La-O2	2.621(3)	La-O5	2.523(3)	La-O8	2.496(3)
La-O3	2.636(3)	La-O6	2.506(3)	La-O9	2.506(3)

Chelate Angles / °					
Atoms 1-2-3	Angle	Atoms 1-2-3	Angle	Atoms 1-2-3	Angle
O1-La-O2	62.43(11)	O1-La-O3	124.17(11)	O2-La-O3	61.84(10)
O4-La-O5	70.42(9)	O7-La-O6	69.11(10)	O8-La-O9	66.90(10)

O-La-O Angles / °					
Atoms 1-2-3	Angle	Atoms 1-2	Angle	Atoms 1-2-3	Angle
O4-La-O1	141.85(10)	O4-La-O2	122.11(10)	O4-La-O3	71.63(10)
O4-La-O6	76.77(10)	O4-La-O8	107.58(11)	O4-La-O9	72.84(10)
O5-La-O1	78.76(10)	O5-La-O2	68.57(10)	O5-La-O3	78.84(10)
O6-La-O1	138.71(11)	O6-La-O2	116.38(11)	O6-La-O3	72.57(10)
O6-La-O5	141.79(10)	/	/	/	/
O7-La-O1	74.25(11)	O7-La-O2	66.61(10)	O7-La-O3	86.89(11)
O7-La-O5	134.52(10)	O7-La-O8	72.23(11)	O7-La-O9	132.92(11)
O8-La-O1	80.72(12)	O8-La-O2	130.25(11)	O8-La-O3	142.21(11)
O8-La-O5	137.84(10)	O8-La-O6	70.66(11)	/	/
O9-La-O1	77.03(11)	O9-La-O2	127.90(11)	O9-La-O3	140.17(10)
O9-La-O5	72.78(10)	O9-La-O6	115.65(11)	/	/

Table S5 Selected Least-Squares Planes Data in a) [La(pbta)₃(dig)] and b) [La(hfa)₃(dig)].^{S4}

a)

Least-Squares Planes		
Least Squares planes description	Abbreviation	Max. deviation/Å
Trifluoroperfluorophenylacetylacetonate O9, O8, C52, C53, C57, C58, C59	pbta1	0.038
Trifluoroperfluorophenylacetylacetonate O4, O8, C16, C17, C21, C22, C23	pbta2	0.030
Trifluoroperfluorophenylacetylacetonate O6, O7, C34, C35, C39, C40, C41	pbta3	0.034

Interplanar angles / ° ^a			
	pbta1	pbta2	pbta3
pbta1		79.9	82.7
pbta2			15.6

^a Typical uncertainties :0.5°

b)

Least-Squares Planes		
Least Squares planes description	Abbreviation	Max. deviation/Å
Hexafluoroacetate C9, C6, C7, C8, O3, O4, C10	hfa1	0.038
Hexafluoroacetate O5, C13, C12, C11, O6, C14, C15	hfa2	0.024
Hexafluoroacetate O2, C3, C2, C1, O1, C4, C5	hfa3	0.009

Interplanar angles / ° ^a			
	hfa1	hfa2	hfa3
hfa1		67.0	93.4
hfa2			71.8

^a Typical uncertainties :0.5°

Table S6 Bond Distances ($\delta_{Ln,j}$), Bond Valences ($v_{Ln,j}$)^a and Total Atom Valence (V_{Ln})^b in the Crystal Structure of [La(pbta)₃(dig)].

Atom	Donor type	$\delta_{Ln,j} / \text{\AA}$	$v_{Ln,j}$	
O1	dig (central)	2.618	0.273	Average O-dig
O2	dig (distal)	2.621	0.271	0.27(1)
O3	dig (distal)	2.636	0.260	
O4	pbta	2.472	0.405	Average O-pbta
O5	pbta	2.523	0.353	0.38(2)
O6	pbta	2.506	0.370	
O7	pbta	2.495	0.381	
O8	pbta	2.496	0.380	
O9	pbta	2.506	0.370	
		V_{Ln}	3.063	

^a $v_{Ln,j} = e^{\left[\frac{(R_{Ln,j} - \delta_{Ln,j})}{b}\right]}$ where $\delta_{Ln,j}$ is the La-donor atom j distance. The valence bond parameters $R_{Ln,O}$ are taken from reference S5 and $b = 0.37 \text{ \AA}$. ^b $V_{Ln} = \sum_j v_{Ln,j}$ ^{S6} Numbering taken from Figure S5.

Table S7 Average Bond Distances (Ln-O_{dig} and Ln-O_{diketone}), Average Bond Valences ($v_{Ln,Odig}$ and $v_{Ln,Odiketone}$)^a and Total Atom Valence (V_{Ln})^b in the Crystal Structures of [La(hfa)₃(dig)],^{S4} [La(pbta)₃(dig)], and [Eu(pbta)₃(dig)].

	[La(hfa) ₃ (dig)]	[La(pbta) ₃ (dig)]	[Eu(pbta) ₃ (dig)]
Ln-O _{dig} / \AA^c	2.55(6)	2.63(1)	2.54(1)
Ln-O _{diketone} / \AA^d	2.53(6)	2.50(2)	2.40(2)
$v_{Ln,Odig}^c$	0.34(6)	0.27(1)	0.26(1)
$v_{Ln,Odiketone}^d$	0.35(6)	0.38(2)	0.37(2)
V_{Ln}	3.111	3.063	3.013

^a $v_{Ln,j} = e^{\left[\frac{(R_{Ln,j} - \delta_{Ln,j})}{b}\right]}$ where $\delta_{Ln,j}$ is the La-donor atom j distance. The valence bond parameters $R_{Ln,O}$ are taken from reference S5 and $b = 0.37 \text{ \AA}$. ^b $V_{Ln} = \sum_j v_{Ln,j}$ ^{S6 c,d} Each values correspond to an average of three^c or six^d bonds and the uncertainties are estimated via standard deviation associated with each averaging.

- (S4) Malandrino, G.; Licata, R.; Castelli, F.; Fragalà, I. L.; Benelli, C., New Thermally Stable and Highly Volatile Precursors for Lanthanum MOCVD : Synthesis and Characterization of Lanthanum β -diketonate Glyme Complexes. *Inorg. Chem.* **1995**, *34*, 6233-6234.
- (S5) (a) Trzesowska, A.; Kruszynski, R.; Bartczak, T. J., New bond-valence parameters for lanthanides. *Acta Cryst B Structural Science* **2004**, *B60*, 174-178; (b)Trzesowska, A.; Kruszynski, R.; Bartczak, T. J., New lanthanide-nitrogen bond-valence parameters. *Acta Cryst B Structural Science* **2005**, *B61*, 429-434; (c) Trzesowska, A.; Kruszynski, R.; Bartczak, T. J., Bond-valence parameters. *Acta Cryst B Structural Science* **2006**, *B62*, 745-753.
- (S6) (a) Brown, I. D., *The Chemical Bond in Inorganic Chemistry*, Oxford University Press, UK, 2002; (b) Brown, I. D., Recent Development in the Methods and Applications of the Bond Valence Model. *Chem. Rev.* **2009**, *109*, 6858-6919.

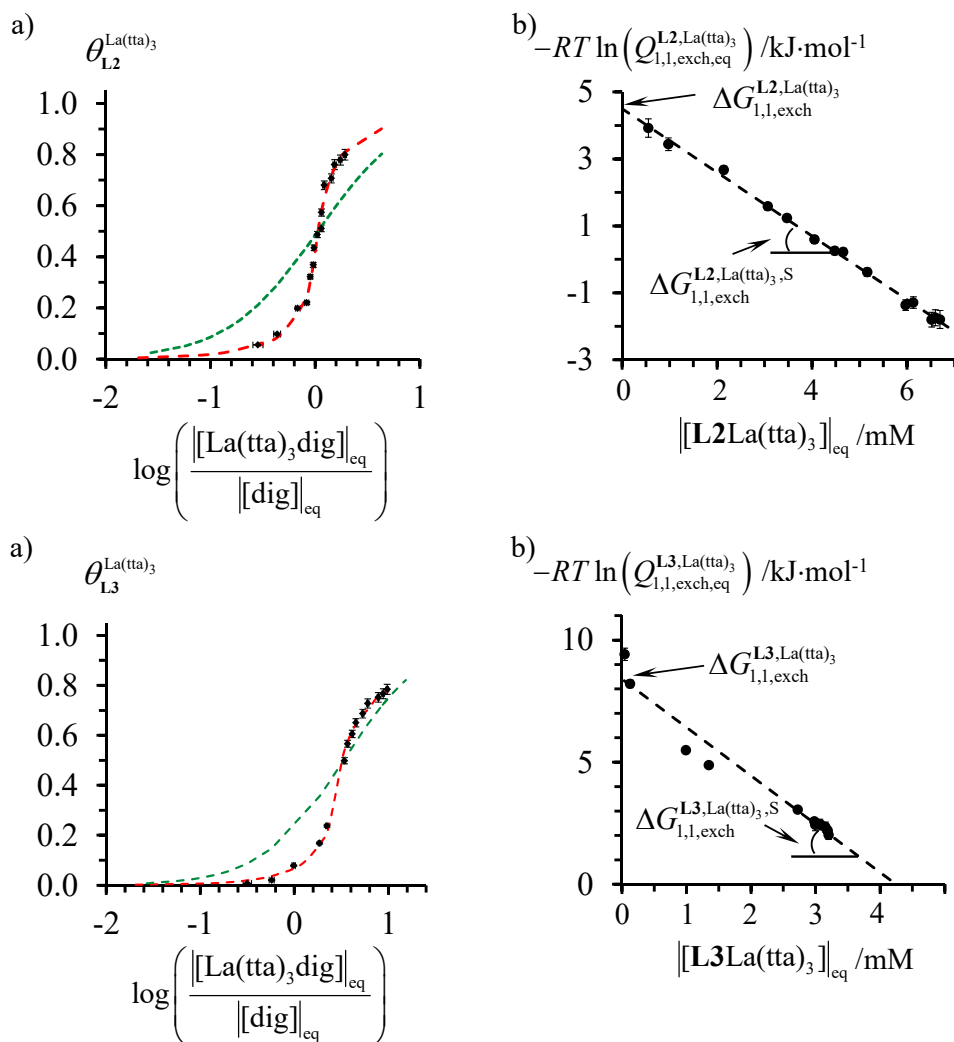


Figure S4 a) Experimental (diamonds) and fitted (dotted green traces using eqn 12; dashed red traces using eqn 13) pseudo-binding isotherms recorded for the 1H -NMR titration of **L2** (top) and **L3** (bottom) with $[La(tta)_3dig]$ in CD_2Cl_2 at 298 K and b) dependence of the equilibrium reaction quotients $-RT \ln(Q_{1,1,exch,eq}^{LK,La(tta)_3})$ with the progress of the association reaction highlighting $\Delta G_{1,1,exch}^{LK,La(tta)_3}$ and $\Delta G_{1,1,exch}^{LK,La(tta)_3,S}$ according to eqn (10).

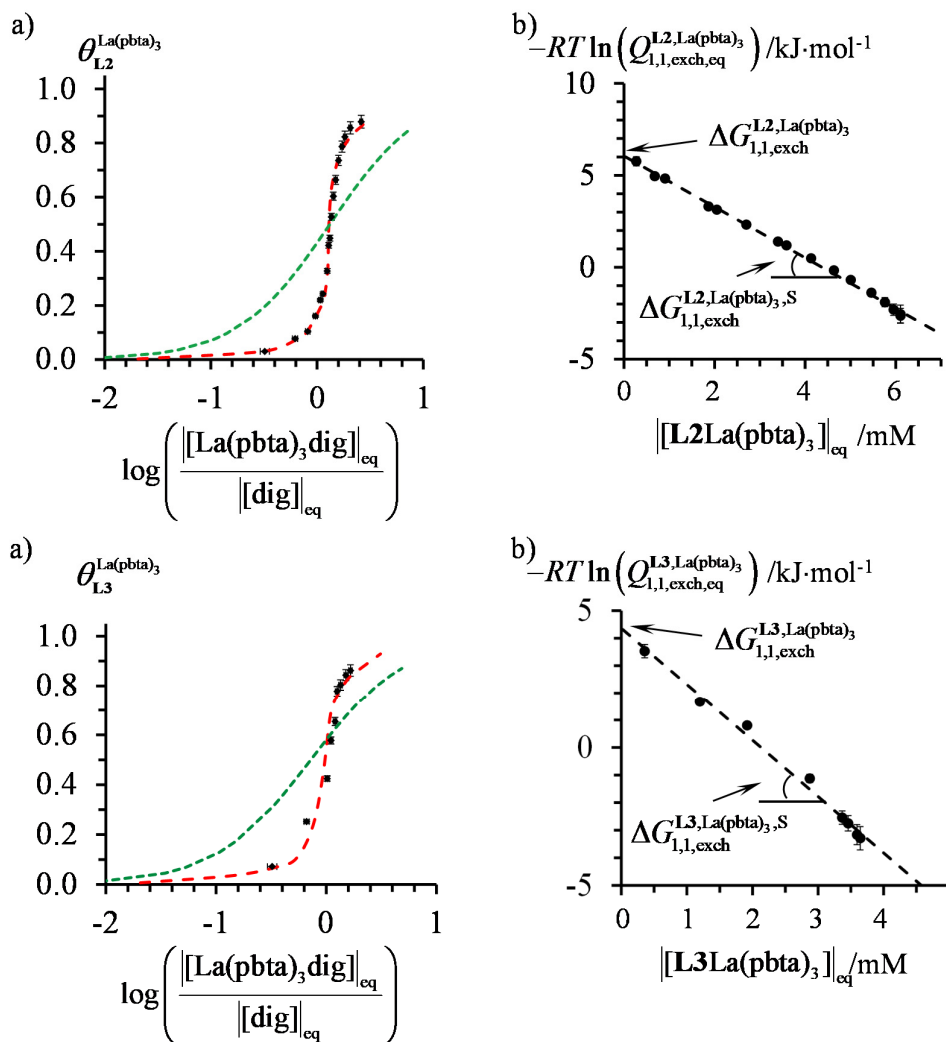


Figure S5 a) Experimental (diamonds) and fitted (dotted green traces using eqn 12; dashed red traces using eqn 13) pseudo-binding isotherms for the $^1\text{H-NMR}$ titration of **L2** (top) and **L3** (bottom) with $[\text{La}(\text{pbta})_3\text{dig}]$ in CD_2Cl_2 at 298 K and b) dependence of the equilibrium reaction quotients $-RT \ln(Q_{1,1,\text{exch,eq}}^{\text{L1,L1,La(pbta)}_3})$ with the progress of the association reaction highlighting $\Delta G_{1,1,\text{exch}}^{\text{L1,L1,La(pbta)}_3}$ and $\Delta G_{1,1,\text{exch}}^{\text{L1,L1,La(pbta)}_3,\text{S}}$ according to eqn (10).

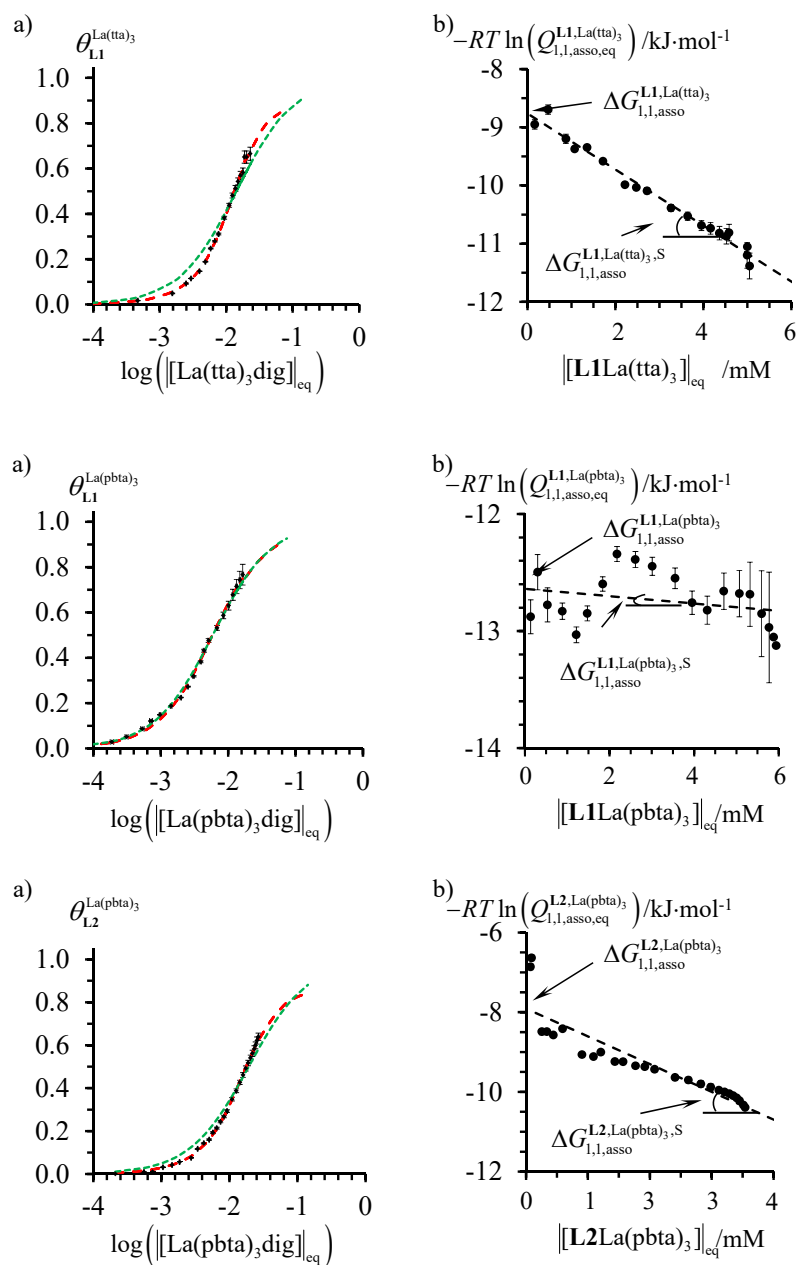


Figure S6 a) Experimental (diamonds) and fitted (dotted green traces using eqn 12; dashed red traces using eqn 13) binding isotherms recorded for the ¹H-NMR titration of **L1** with [La(tta)₃dig] (top), **L1** with [La(pbta)₃dig] (middle) and **L2** with [La(pbta)₃dig] (bottom) in CD₂Cl₂ + 0.14 M diglyme at 298 K and b) dependence of the equilibrium reaction quotients $-RT \ln(Q_{1,1,exch,eq}^{Lk,La(X)_3})$ with the progress of the association reaction highlighting $\Delta G_{1,1,exch}^{Lk,La(X)_3}$ and $\Delta G_{1,1,exch}^{Lk,La(X)_3,S}$ according to eqn (10).

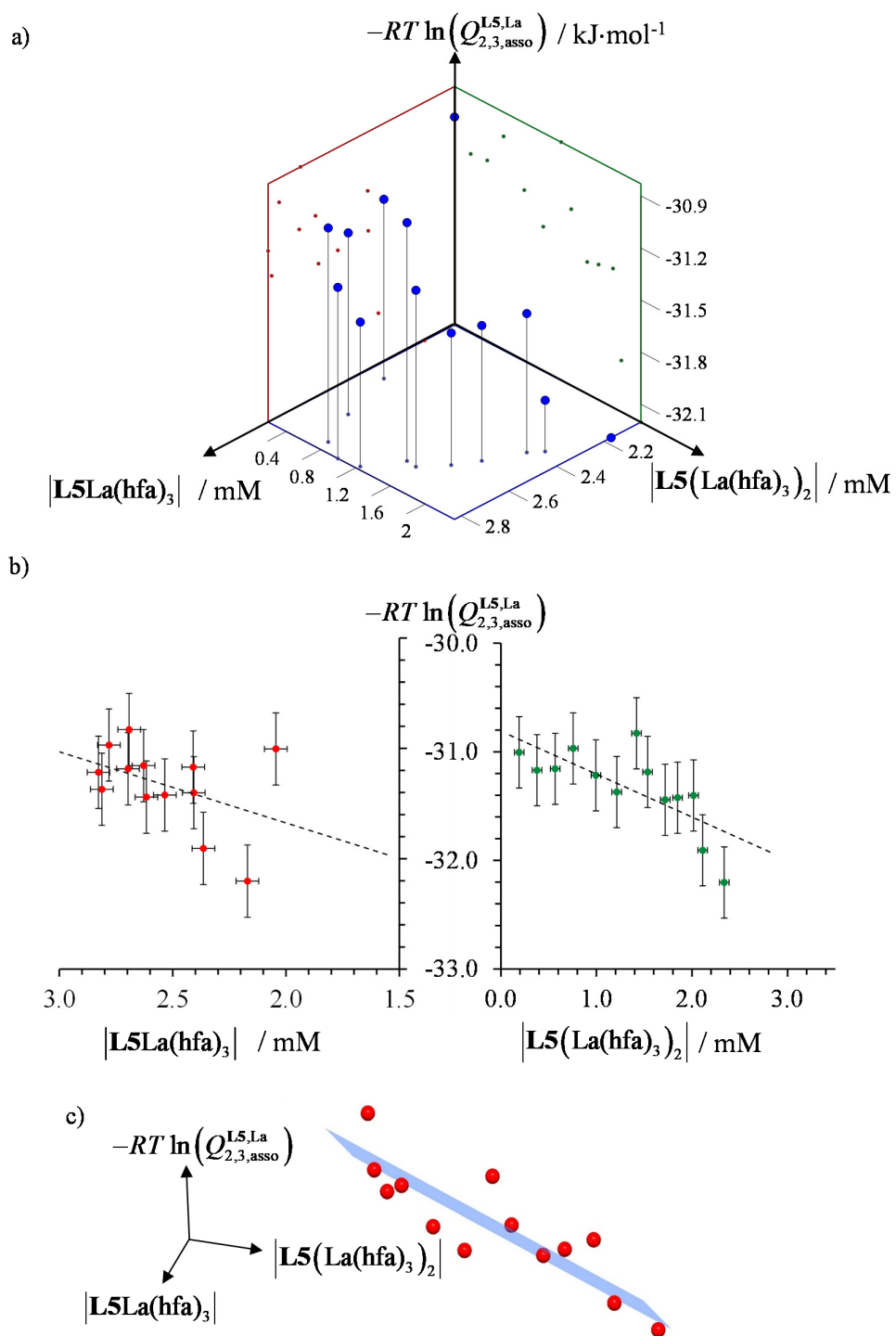


Figure S7 Plots of a) $-RT \ln(Q_{2,3,asso,eq}^{L5,La})$ as a function of $|L5La(hfa)_3|_{eq}$ and $|L5(La(hfa)_3)_2|_{eq}$ according to eqn (26), b) projections onto the $|L5(La(hfa)_3)_2|_{eq} = \text{constant}$ plane (left) and $|L5La(hfa)_3|_{eq} = \text{constant}$ plane (right) and c) projection roughly orthogonal to the best least-square plane (shown in blue) for the titrations of **L5** with $[La(hfa)_3]_{dig}$ in CH_2Cl_2 + 0.14 M diglyme (298 K).

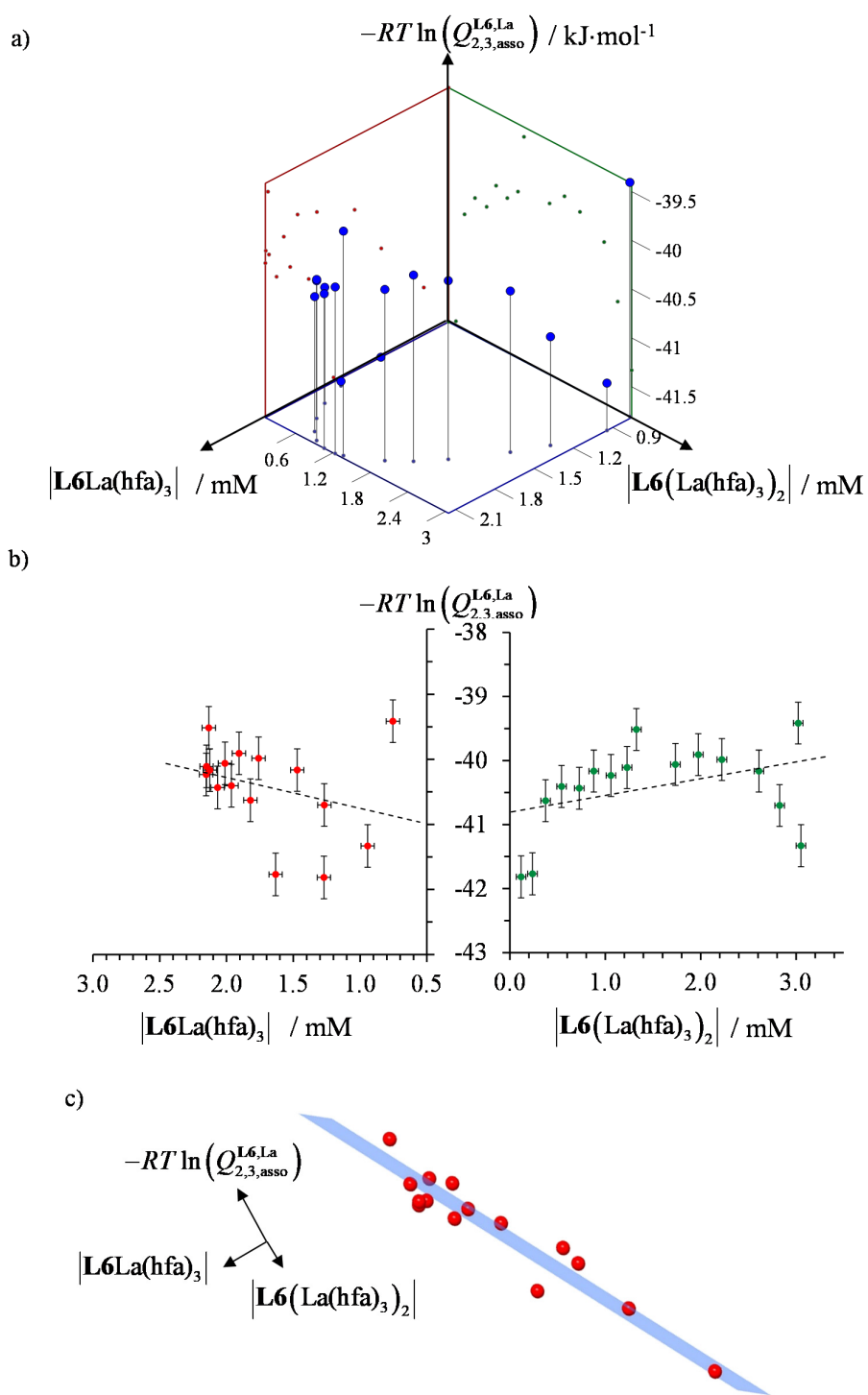


Figure S8 Plots of a) $-RT \ln(Q_{2,3,asso,eq}^{L6,La})$ as a function of $[L6La(hfa)_3]_{eq}$ and $[L6(La(hfa)_3)_2]_{eq}$ according to eqn (26), b) projections onto the $[L6(La(hfa)_3)_2]_{eq} = \text{constant}$ plane (left) and $[L6La(hfa)_3]_{eq} = \text{constant}$ plane (right) and c) projection roughly orthogonal to the best least-square plane (shown in blue) for the titrations of **L6** with $[La(hfa)_3\text{dig}]$ in CD_2Cl_2 + 0.14 M diglyme (298 K).

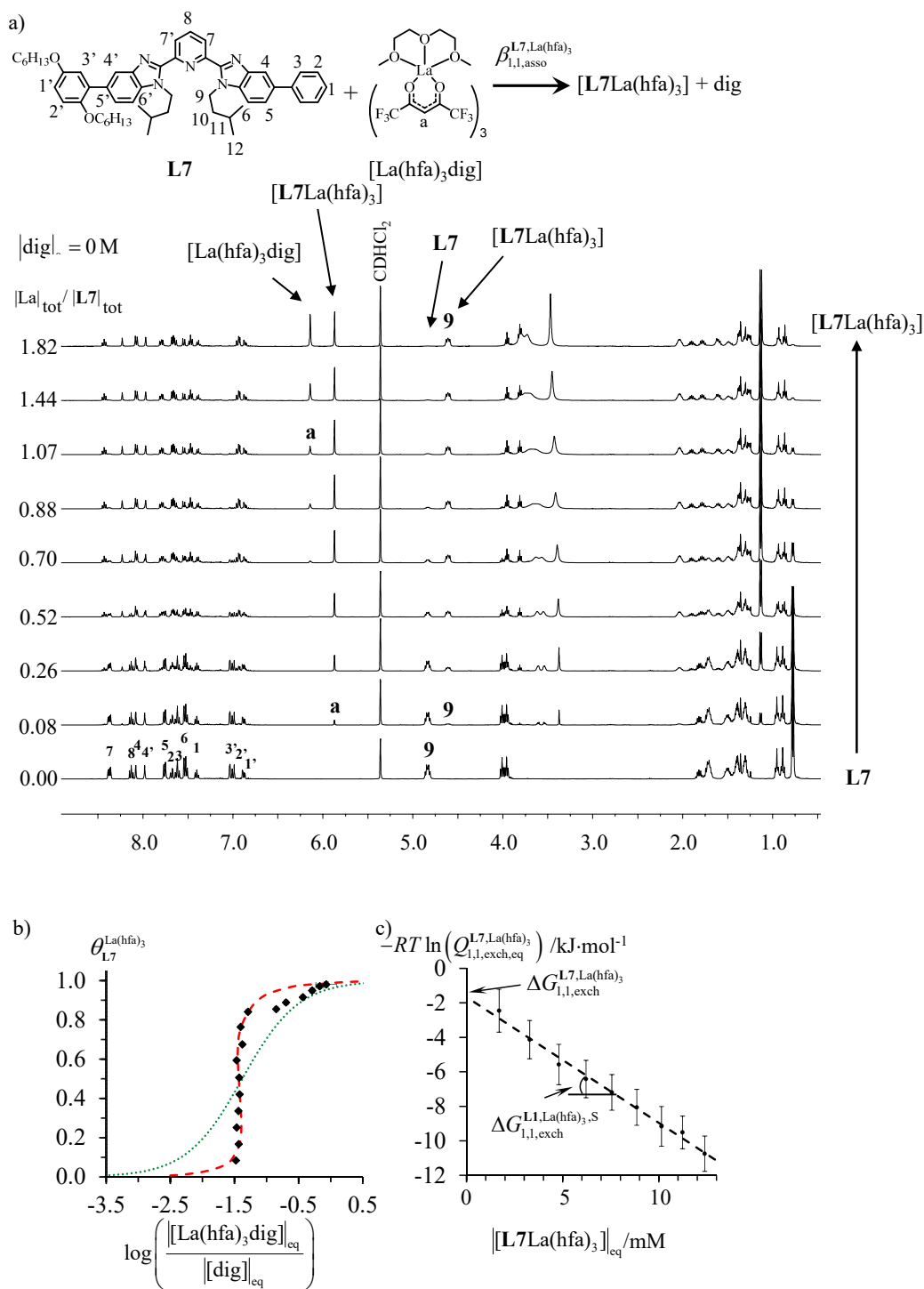


Figure S9 a) $^1\text{H-NMR}$ titration of **L7** with $[\text{La}(\text{hfa})_3]\text{dig}$ in CD_2Cl_2 at 298 K with numbering scheme, b) experimental (diamonds) and fitted (dotted green traces using eqn 12; dashed red traces using eqn 13) binding isotherms and c) dependence of the equilibrium reaction quotients $-RT \ln(Q_{1,1,\text{exch},\text{eq}}^{\text{L7,La}(\text{hfa})_3})$ on the progress of the association reaction highlighting $\Delta G_{1,1,\text{exch}}^{\text{L7,La}(\text{hfa})_3}$ and $\Delta G_{1,1,\text{exch}}^{\text{L1,La}(\text{hfa})_3,\text{S}}$ according to eqn (10).

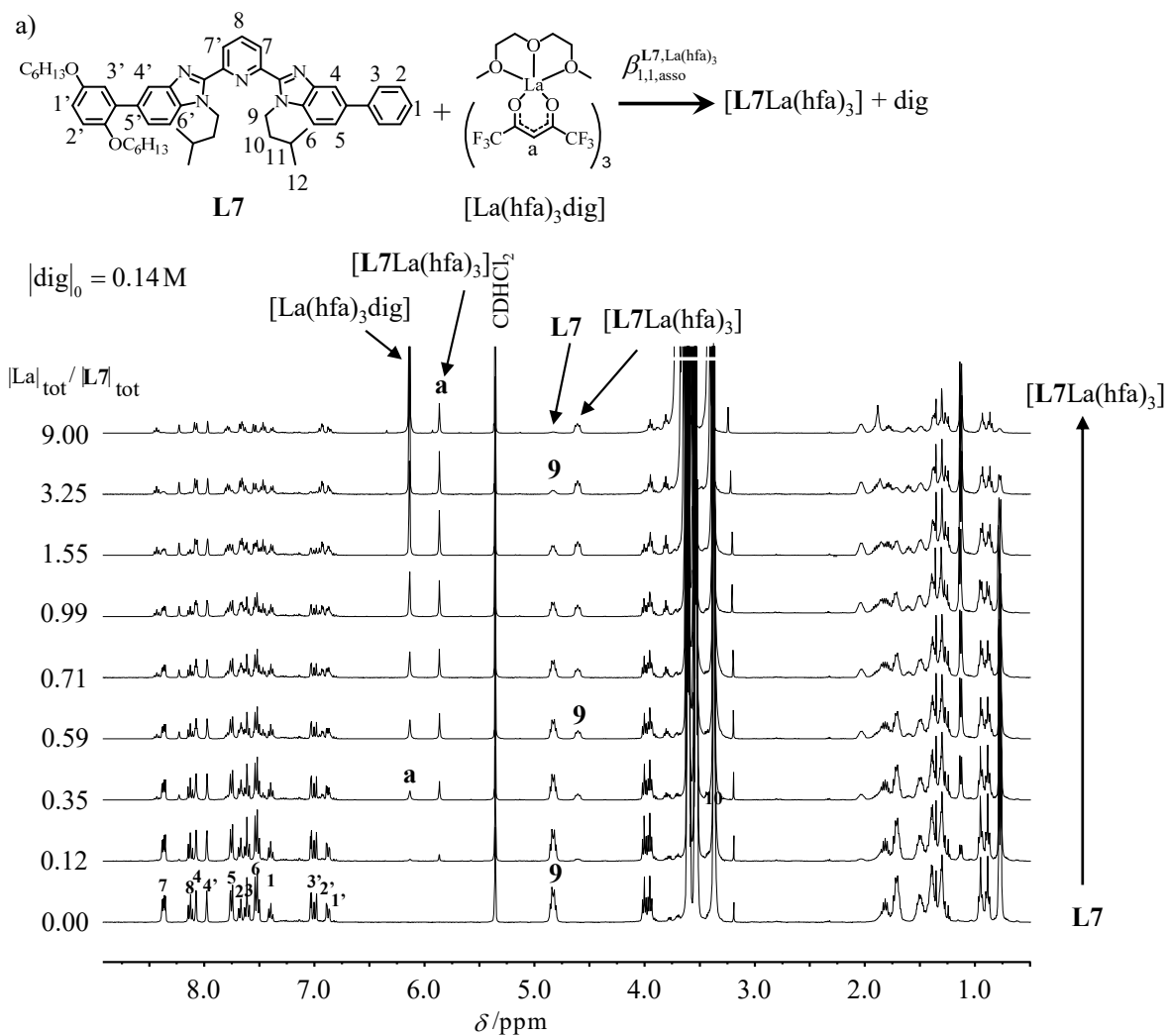


Figure S10 ^1H -NMR titration of **L7** with $[\text{La}(\text{hfa})_3]\text{dig}$ in $\text{CD}_2\text{Cl}_2 + 0.14 \text{ M}$ diglyme at 298 K with numbering scheme.

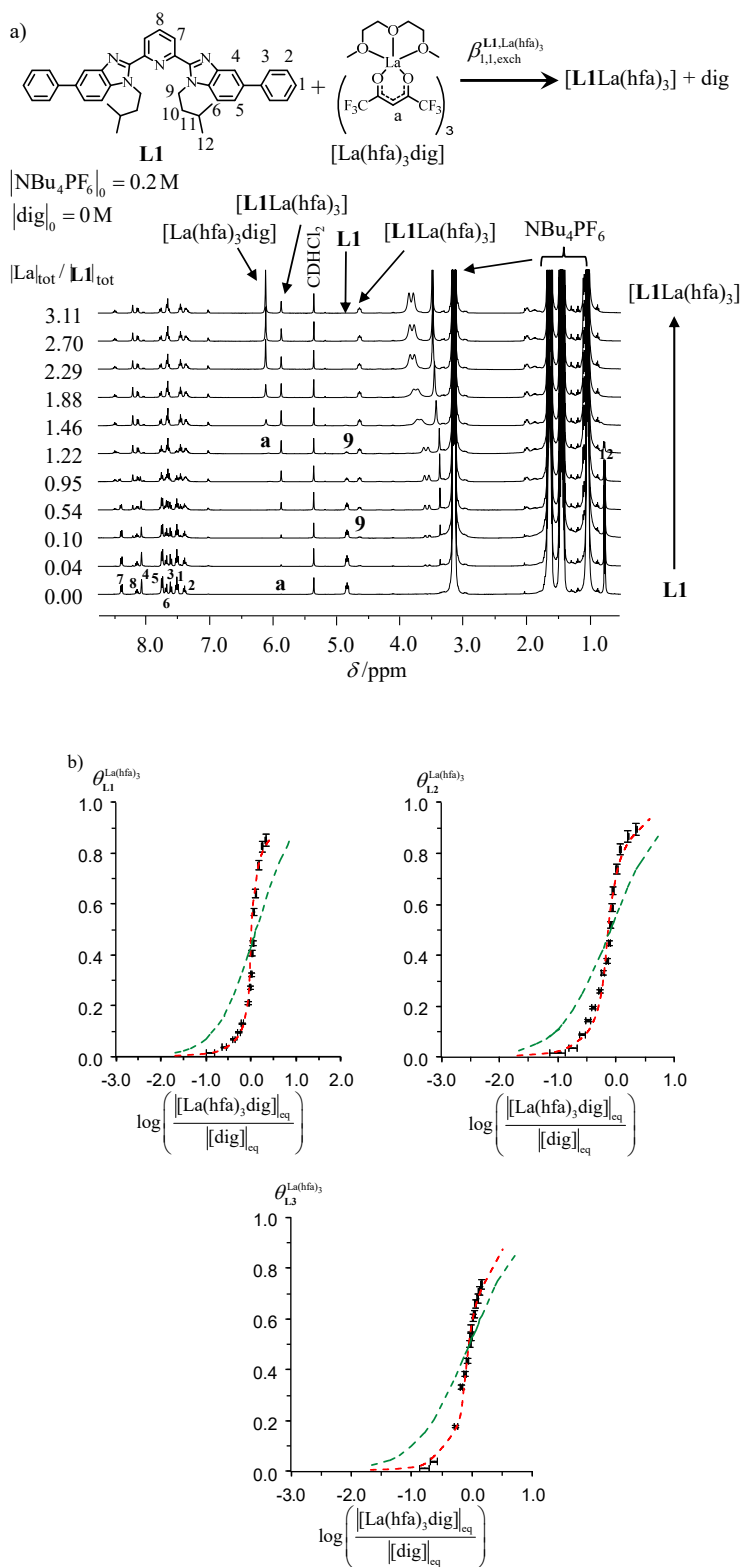


Figure S12 a) ^1H -NMR titration of **Lk** with $[\text{La}(\text{hfa})_3]\text{dig}$ in $\text{CD}_2\text{Cl}_2 + 0.2\text{ M NBu}_4\text{PF}_6$ at 298 K with numbering scheme, b) experimental (diamonds) and fitted (dotted green traces using eqn 12; dashed red traces using eqn 13) binding isotherms for **L1-L3**.

Table S8 Average Free Energies $-RT \ln(\beta_{1,1}^{\text{Lk,La}})$ (eqns 8 and 12) and Thermodynamic Parameters $\Delta G_{1,1}^{\text{Lk,La}}$ and $\Delta G_{1,1}^{\text{Lk,La,S}}$ (eqn 10), Determined for the Titrations of **Lk** with [La(hfa)₃dig] in in Pure CD₂Cl₂ (eqn 6) and in Presence of Additional 0.2 M of benzene (C₆H₆) or NBu₄PF₆.^a

Hosts	Spectators	$-RT \ln(\beta_{1,1}^{\text{Lk,La}})$	$\Delta G_{1,1}^{\text{Lk,La}}$	$\Delta G_{1,1}^{\text{Lk,La,S}}$
		/kJ·mol ⁻¹	/kJ·mol ⁻¹	/kJ·mol ⁻¹
L1	none	-4.6(2.1)	5.9(3)	-1615(50)
L1	C ₆ H ₆	1.1(2.1)	6.0(2)	-1198(54)
L1	NBu ₄ PF ₆	0.0(2.4)	5.4(1)	-1144(19)
L2	none	-3.4(2.7)	5.6(3)	-1503(71)
L2	C ₆ H ₆	-1.8(1.6)	2.1(2)	-832(45)
L2	NBu ₄ PF ₆	-1.0(2.2)	3.6(2)	-1168(46)
L3	none	-3.9(2.4)	4.0(3)	-2020(92)
L3	C ₆ H ₆	-0.2(1.2)	3.9(1)	-1540(34)
L3	NBu ₄ PF ₆	-0.3(1.3)	4.1(3)	-1716(116)

^aUncertainties are those obtained by least-square fits using eqns (8) and (10).

Table S9 Average Free energies $-RT \ln(\beta_{1,1}^{Lk,La})$ (eqns 8 and 12) and Thermodynamic Parameters $\Delta G_{1,1}^{Lk,La}$ and $\Delta G_{1,1}^{Lk,La,S}$ (eqn 10), Determined for the Titrations of **Lk** with [La(hfa)₃dig] in in CD₂Cl₂ + 0.14 M diglyme and in Presence of Additional 0.2 M of Benzene (C₆H₆) or NBu₄PF₆.^a

Hosts	Spectators	$-RT \ln(\beta_{1,1}^{Lk,La})$	$\Delta G_{1,1}^{Lk,La}$	$\Delta G_{1,1}^{Lk,La,S}$
		/kJ·mol ⁻¹	/kJ·mol ⁻¹	/kJ·mol ⁻¹
L1	none	-13.2(6)	-12.2(1)	-305(22)
L1	C ₆ H ₆	-12.2(4)	-11.3(1)	-264(29)
L1	NBu ₄ PF ₆	-14.2(1)	-12.3(3)	-436(64)
L2	none	-9.8(6)	-8.8(1)	-254(24)
L2	C ₆ H ₆	-9.7(2)	-9.2(1)	-312(67)
L2	NBu ₄ PF ₆	-15.5(6)	-12.4(2)	-1072(77)
L3	none	-9.5(8)	-9.0(1)	-285(36)
L3	C ₆ H ₆	-9.6(2)	-9.3(1)	-552(49)
L3	NBu ₄ PF ₆	-12.8(7)	-10.8(2)	-855(95)

^aUncertainties are those obtained by least-square fits using eqns (8) and (10).